PERGAMON

International Journal of Heat and Mass Transfer 45 (2002) 1467–1475

International Journal of HEAT and MASS TRANSFER

www.elsevier.com/locate/ijhmt

Direct contact melting of porous material

Hiroyuki Kumano *, Akio Saito, Seiji Okawa

Department of Mechanical Sciences and Engineering, Graduate School of Science and Engineering, Tokyo Institute of Technology, 2-12-1 Ookayama, Meguro-ku, Tokyo 152-8552, Japan

Received 8 November 2000; received in revised form 6 July 2001

Abstract

The direct contact melting of a porous material is investigated experimentally and analytically. The phase change material (PCM) is made of fine ice particles of a nearly uniform diameter, which is changed as a parameter. In the analysis, two models are proposed. One is calculated as the direct contact melting of a monolithic sample and another is treated as an assembly of the direct contact melting of the individual particles. As a result, it was found that the heat flux increased with the diameter, due to increase of permeability in a case of small diameter. But, in a case of large diameter, the heat flux decreased as the particle diameter increased because the direct contact melting occurred independently for the individual particles.

1. Introduction

Melting of a porous material is a very important phenomenon occurring in several engineering processes. In a dynamic type ice thermal energy storage system, which is a method of the load leveling of electric power, ice particles with fluidity are often used as the thermal storage material. In such cases, the ice particles often form a porous material in the system. Melting of a porous material is also a fundamental process in chemical engineering. The melting process of the porous material must be considered for understanding the characteristics of these systems.

In past studies of melting process of a porous material, Kearns and Plumb [1] measured the melting behavior in the porous material experimentally, when the porous material was melted on a heating plate. Aoki et al. [2] examined a melting process for a snow layer with permeation of melted liquid into the snow.

When a heating plate and the phase change material (PCM) are pressed against each other, melted liquid is squeezed out through a thin liquid film formed between the solid surface and the heating plate. Since heat is exchanged across this thin liquid film, a high heat flux can be obtained compared with a heat transfer, for example, dominated by natural convection. This phenomenon is known as the direct contact melting and appears in a thermal energy storage capsule utilizing the latent heat. Over the past decade, many researchers have attempted to investigate the characteristics of the direct contact melting [3–6]. The phenomenon pressing a cylindrical solid onto a plate was first investigated experimentally and analytically by Saito et al. They showed a relation among the heat flux, the Stefan number and the pressing force using non-dimensional parameters in Trans. JSME., 1984. It was translated into English in 1985 [3–5]. Later, Moallemi et al. [6] reported a similar relation in 1986.

In the present study, melting phenomena of porous materials are investigated from a view point of direct contact melting, experimentally and analytically. The effects of the size of particles are considered. In the analysis, two models are proposed and the validity and the applicable range of each model are examined.

2. Experiment

2.1. Experimental apparatus and conditions

Fig. 1 illustrated the main apparatus. The system consists of the main apparatus, a constant temperature

* Corresponding author.
E-mail address: kumano@mech.titech.ac.jp (H. Kumano).

0017-9310/02/$ - see front matter
PII: S0017-9310(01)00241-1

Nomenclature

c	specific heat of liquid (J/(kg K))
g	gravitational acceleration (m/s^2)
h	height of permeation layer (m)
H_{eq}	equilibrium height of permeation layer (m)
H_0	height of the water surface from the bottom of the porous material (m)
k	permeability (m^2)
L	latent heat of melting (J/kg)
M	mass of solid (kg)
p_l	pressure in liquid film (Pa)
p_p	pressure in porous material (Pa)
P_c	driving pressure (Pa)
P_L	average pressure due to the gravitational force of the weight (Pa)
P_S	average pressure due to the gravitational force of the sample (Pa)
q	heat flux (W/m^2)
r, z	coordinates (m)
R	radius of sample (m)
Ste	Stefan number based on the heating plate temperature ($c(T_s - T_m)/l$)
Ste'	Stefan number based on the brine temperature ($c(T_{br} - T_m)/l$)
t	time (s)
T_{br}	brine temperature (°C)
T_m	melting point (°C)
T_s	temperature at the top surface of the heating plate (°C)
u	velocity in r-direction (m/s)
v	velocity in z-direction (m/s)
V_c	interface velocity of permeation layer (m/s)
W	mass of weight (kg)

Greek symbols

ε	porosity
δ	thickness of liquid film (m)
λ	thermal conductivity of liquid (W/(m K))
μ	viscosity of liquid (Pa s)
ρ	density of liquid (kg /m^3)

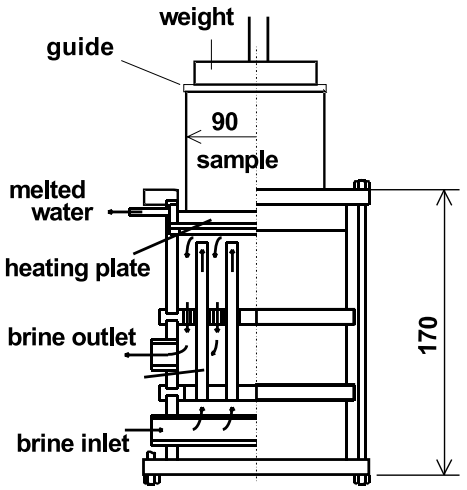

Fig. 1. Experimental apparatus.

bath and measuring instruments. A cylindrical sample was placed on a circular heating plate set horizontally. A load pressing the sample on the heating plate was the sum of gravitational forces due to the sample itself and a weight placed on the sample. The heating plate was made of copper 100 mm in diameter and 16 mm in thickness. The surface temperature of the heating plate was adjusted by controlling brine temperature circulating beneath the heating plate. The brine temperature was maintained at a constant value through the experiment using the constant temperature bath. Three sets of T-type thermocouples were installed in the heating plate as shown in Fig. 2. One set consisted of two thermocouples, which were located at 2 mm depth from each surface. Three sets were installed at locations 25 mm from the center of the heating plate in 120° intervals in the angular direction. The temperature of the heating plate was measured by these thermocouples. The top and bottom surface temperatures were calculated from these values. A guide was placed on the sample to make the sample move vertically and to assure the force due to the weight acted on the top of the sample uniformly. Variation of a sample height was measured at 15 s intervals by a caliper which moves with the guide. Average pressure due to the load and the amount of melting were calculated from the height and its variation, respectively.

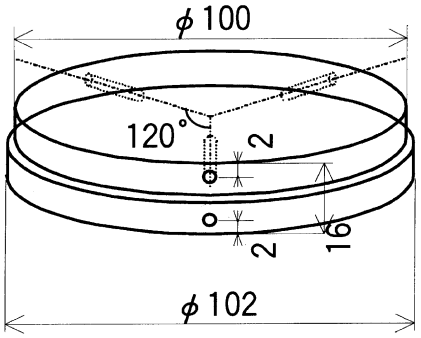

Fig. 2. Details of the heating plate.

In past studies, authors showed that dimensionless heat flux obtained from experiments was a function of the *Ste* based on the heating plate temperature and average pressure due to the load. When a dense solid is used as the PCM, the surface temperature can be easily controlled to a constant value throughout a experiment and the phenomenon can be treated as a quasi-steady. Hence, in many studies of the direct contact melting, the *Ste* is used as a key parameter.

In the present study, the measurements were carried out including a time before reaching the quasi-steady state in order to examine transient effects of the diameter of the particles forming the sample. For this reason, the variation of heat flux through the heating plate is larger than that of the melting process of a dense solid, and it is difficult to keep the surface temperature constant and to define the *Ste* on the basis of the surface temperature. Therefore, the brine temperature was kept at a constant value through the experiment. Then, the Ste' was introduced, which is the Stefan number based on the difference between the brine temperature and the melting point. The brine temperature is set at 16 °C and the *Ste* defined by the surface temperature was varied in the range from 0.05 to 0.12. Total load, determined by a sum of the mass of the sample and the weight, decreases with the melting of the sample. The symbol P_L is the average pressure due to the mass of the weight and it is defined as the mass of the weight per cross-sectional area of the sample. The average pressure due to the mass of the weight, P_L, is set at 7.67×10^2 Pa. Since the mass of the sample decreases with the melting, the average pressure due to the mass of the sample was varied in the range from 0 to 3.9×10^2 Pa.

2.2. Method of making the samples and measuring the property of the porous material

Table 1 shows the particle diameter, porosity, permeability and driving pressure by capillary effect at each sample. Six samples were examined. After the ice particles were made by breaking block ices into pieces. These were sized using sieves and then pressed in a cylindrical vessel 90 mm in diameter and 100 mm in height. These operations were carried out in a constant temperature room kept at −2 °C. The porosity was calculated from the mass and the volume of the sample. After these were kept in a refrigerator set at 0 °C for several hours, the samples were used in the experiments.

When a porous material is melted, permeation of melted liquid into the porous material must be considered. Properties of the porous material are very important for understanding the phenomenon. The permeability and the driving pressure were measured using apparatus shown in Fig. 3. A cylinder of 36 mm in diameter was filled with the ice particles, and it was placed on a shallow vessel filled with water. Time dependency of a height of the permeation layer was measured using a video camera. The following relationship [7] among a permeation velocity, a permeability and a driving pressure were used to determine k and P_c.

$$V_c = \frac{dh}{dt} = -\frac{k}{\varepsilon\mu}\frac{\rho g(h - H_{eq})}{h}, \tag{1}$$

$$H_{eq} = -\frac{P_c}{\rho g} + H_0. \tag{2}$$

Fig. 4 shows the relationship between the height of the permeation layer and time. Symbols indicate the

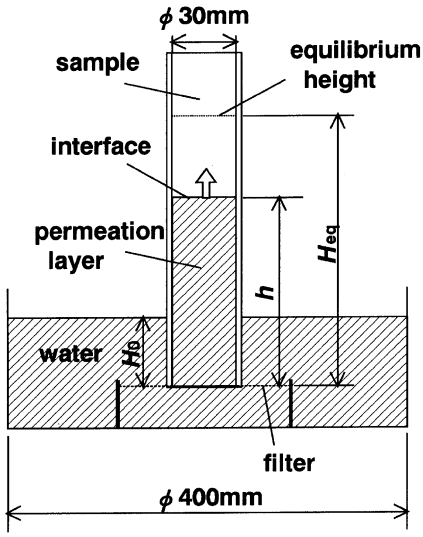

Fig. 3. Experimental apparatus for measuring permeability.

Table 1
Properties of porous materials

Sample	Particle diameter (mm)	Porosity ε	Permeability k (m^2)	Driving pressure P_c (Pa)
1	~0.5	0.438	1.15×10^{-12}	-3.42×10^4
2	0.5–1.0	0.464	1.05×10^{-10}	-1.02×10^3
3	1.7–2.8	0.441	6.9×10^{-10}	-2.84×10^2
4	2.8–4.0	0.449	1.35×10^{-9}	-1.76×10^2
5	4.0–6.7	0.370		
6	10–20	0.393		

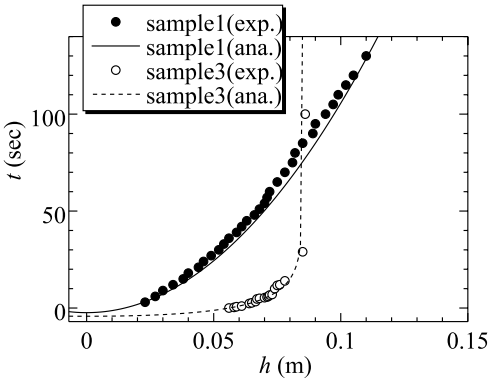

Fig. 4. Relationship between the interface height and time.

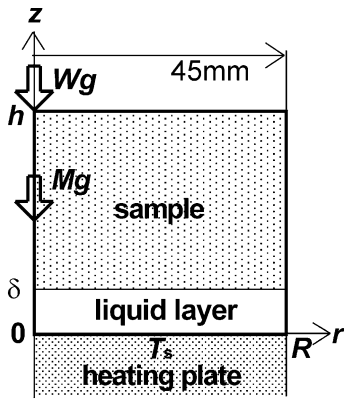

Fig. 5. Melting model on the cross-section of the sample.

experimental results and the lines are calculated using Eq. (1), for the properties shown in Table 1. The experimental and analytical values show good agreement. It is found that the properties were appropriately determined for each sample. Since the height of the permeation layer was uniform in the radial direction in the experiments, the property distributions in the sample are assumed to be uniform.

3. Analysis

In this paper, effects of the particle diameter on the melting process of a porous material are considered. The mechanism of the melting process is assumed to be dependent on the particle diameter. Two analytical models are proposed. One is a melting model considering the total cross-section of the sample, the other is a melting model considering individual particles. Calculations were carried out to determine the validity of the analytical models and to confirm the applicable range of each model.

3.1. Melting model considering the total cross-section of the sample

The system was formulated in two-dimensional cylindrical co-ordinates. The calculation was carried out for a melting process with permeation of the melted liquid into the porous material. Fig. 5 shows the physical model. Governing equations were derived under following assumptions.

1. Momentum term of flow is negligible.
2. Pressure in the liquid film is independent of the z-direction.
3. Temperature in the PCM is uniform and at the melting point.
4. Heat transfer in the liquid film is dominated by heat conduction.
5. Melting process is treated as a quasi-steady state for the instantaneous plate temperature and a liquid film thickness.
6. Heat loss to the surroundings is negligible.
7. Flow in the porous material is governed by the Darcy's law.

In previous studies, the analytical solution obtained using the assumptions (1–5) agreed well with the experimental result if the *Ste* is lower than 0.1. For a range of the *Ste* from 0.1 to 0.23, the accuracy of the solution is within ±5%. Therefore, assumptions (1–5) are considered appropriate. Moreover, since run time of the experiment was less than 200 s, assumption (6) is also considered appropriate.

Considering the boundary conditions, the melting process was classified into two situations. Fig. 6 shows schematic diagrams of these situations. Situation 1 is the process until the interface of the permeation layer reaches the top of the sample, and situation 2 is after reaching.

Governing equations and boundary conditions based on the above assumptions are as follows:

In the liquid film

- momentum equation in the r-direction:

$$\frac{\partial p_l}{\partial r} = \mu \frac{\partial^2 u}{\partial z^2}, \tag{3}$$

- momentum equation in the z-direction:

$$\frac{\partial p_l}{\partial z} = 0, \tag{4}$$

- heat flux through the liquid film:

$$q = \lambda \frac{T_s - T_m}{\delta}, \tag{5}$$

- boundary conditions:

$$r = 0: \quad \frac{\partial p_l}{\partial r} = 0, \tag{6}$$

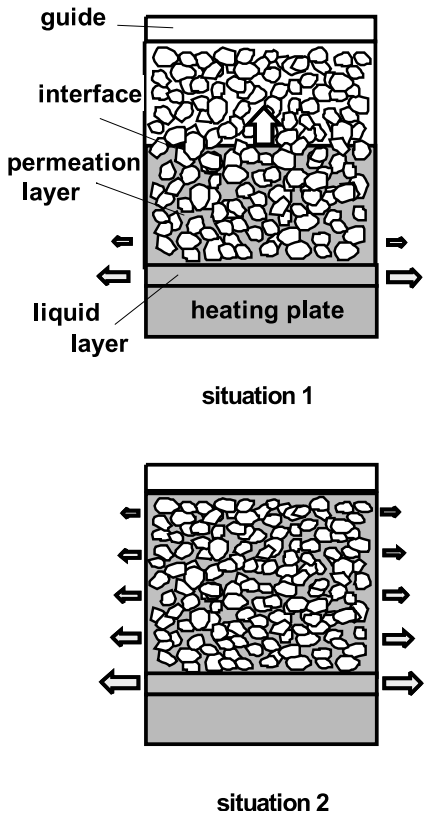

Fig. 6. Situation for each melting process.

$$r = R: \quad p_l = 0, \tag{7}$$

$$r = 0, \delta: \quad u = 0. \tag{8}$$

In the porous material

- continuity equation:

$$\frac{1}{r}\frac{\partial(ru)}{\partial r} + \frac{\partial v}{\partial z} = 0, \tag{9}$$

- momentum equation in the r-direction:

$$u = -\frac{k}{\mu}\frac{\partial p_p}{\partial r}, \tag{10}$$

- momentum equation in the z-direction:

$$v = -\frac{k}{\mu}\left(\frac{\partial p_p}{\partial z} + \rho g\right), \tag{11}$$

- boundary conditions:
  situation 1

$$r = 0: \quad \frac{\partial p_p}{\partial r} = 0, \tag{12}$$

$$r = R: \quad \text{if } p_p \text{ is smaller than } 0, \ \frac{\partial p_p}{\partial r} = 0, \tag{13}$$

$$\text{if } p_p \text{ is larger than } 0, \ p_p = 0, \tag{14}$$

$$z = \delta: \quad p_p = p_l, \tag{15}$$

$$z = h: \quad p_p = P_c, \tag{16}$$

situation 2

$$r = 0: \quad \frac{\partial p_p}{\partial r} = 0, \tag{17}$$

$$r = R: \quad p_p = 0, \tag{18}$$

$$z = \delta: \quad p_p = p_l, \tag{19}$$

$$z = h: \quad \frac{\partial p_p}{\partial z} = 0, \tag{20}$$

- force balance equation:

$$2\pi \int_0^R p_l r \, dr = g(M + W). \tag{21}$$

The temperature of the melted liquid is considered slightly higher than the melting point. But the temperature is estimated to be from 2 to 3 °C, because the temperature of the heating plate is from 4 to 8 °C. Then, although the melting due to the permeation of the liquid occurs in the porous material, the amount of the melting is about 3% of the solid when the pores are filled with the melted liquid. Therefore, the energy equation in the porous material is negligible.

In situation 1, a driving pressure due to the capillary effect acts at the interface of the permeation layer. If a pressure in the porous material is smaller than 0 near the side of the sample, the pressure gradient becomes 0 due to the capillary effect. But, if pressure near the side of the sample is larger than 0, the pressure is set approximately to 0 at the side for a free flow from the sample to the outside. It was assumed that the height of the permeation layer formed by the melted liquid is uniform in the radial direction. In situation 2, a pressure gradient is set to 0 at the top of the sample.

It was assumed that the melting process progresses in a quasi-steady state, maintaining the force balance between the load and the pressure in the liquid film at every moment. Therefore, unsteady terms are not included in these equations. However, variation of mass of the sample must be considered, since the mass decreases with time. Thus, using heat flux obtained at each moment, the variation of the mass in a finite difference of time and the mass at the next time step were calculated. Then, M in Eq. (21) was defined as a total amount of the mass of the permeating liquid and the porous material.

The direct contact melting progresses keeping the force balance between the pressure in the liquid film and the load. In a melting process of a dense solid, the melted liquid flows out through the thin liquid film, and pressure in the liquid film is calculated from the flow rate in the liquid film. But, in a melting process of a porous material, the melted liquid flows out through the liquid film and the porous material. Therefore, in the present

study, the melted liquid permeating into the porous material must be considered. The amount of the melted liquid was determined using a relationship between the surface temperature and the thickness of the liquid film. The amount of the flow permeating into the porous material was computed based on Darcy's law, using the pressure in the liquid film and the boundary conditions. Amount of the melted liquid which flows out through the liquid film was determined by subtracting the amount of the flow permeating into the porous material from the amount melted. The pressure in the liquid film was determined by the amount of flow in the liquid film and the thickness of the liquid film. For the above reasons, all values including the melting amount, the amount of the melted liquid permeating into a porous material and the pressure in the liquid film, must satisfy the governing equations simultaneously, although these were not determined independently. Therefore, the calculation was carried out, varying the values slightly in an iteration of each time step. The iteration was continued for each time step until all values satisfy the governing equations. Then, the calculation progressed to the next time step.

Given the surface temperature obtained from the experiment and the initial height of the sample, time dependency of heat flux was calculated.

3.2. Melting model considering the individual particles

In this model, the system was treated as an assembly of the direct contact melting of individual particles. Fig. 7 shows the analytical model. Assumptions (1–6) explained in Section 3.1 are also applicable to this model. Using the assumptions (1–6), governing equations were derived. Since the particles can be considered as a dense solid, flow in the porous material was not considered here.

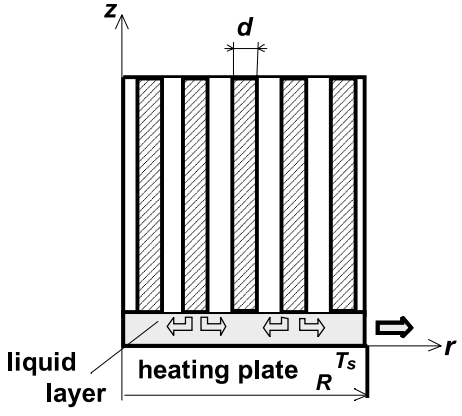

Fig. 7. Melting model considering the individual particles.

Melting velocity, which was derived from an analytical solution obtained under assumptions (1–5), is as follows [3–5]:

$$V_{\mathrm{melt}} = \left[\frac{2\alpha^3 Ste^3}{3\mu R^2}\right]^{0.25} (P_{\mathrm{S}} + P_{\mathrm{L}})^{0.25}. \tag{22}$$

In this model, the porous material is assumed to consist of an assembly of cylinders, the diameters of which are equal to those of the particles. If N is the number of the particles in contact with the heating surface, N is expressed as follows by using the porosity, the diameter of the particles and a radius of the porous material:

$$N = \frac{4R^2(1-\varepsilon)}{d^2}. \tag{23}$$

Considering that Eq. (22) can be applied to each particle, a relation among the melting velocity, the surface temperature and the average pressure can be obtained by substituting Eq. (23) into Eq. (22),

$$V_{\mathrm{melt}} = \left[\frac{8\alpha^3 Ste^3}{3\mu d^2}\right]^{0.25} \left(\frac{P_{\mathrm{S}} + P_{\mathrm{L}}}{N}\right)^{0.25}. \tag{24}$$

Moreover, using Eq. (24), the heat flux can be obtained as follows:

$$q = L\rho(1-\varepsilon)V_{\mathrm{melt}}. \tag{25}$$

Since the melting velocity is affected by the largest particle in the porous material, the particle diameter d was decided as the largest value in the range of the particle diameters. In the case of the direct contact melting for the individual particles, it is considered that a driving pressure within the porous material is very small. Therefore, a pressure due to the gravitational force of the porous material was calculated, neglecting the mass of the permeation layer.

Given the surface temperature obtained from the experiment and the initial height of the sample, the heat flux was calculated as a function of time.

4. Results and discussion

4.1. Experimental results

Fig. 8 shows time dependencies of the heat flux and the temperature at the top surface of the heating plate with the particle diameter of the sample varied as a parameter. Sample 1, 2 and 3 are used. The symbols and the solid lines show the experimentally obtained heat flux and surface temperature for each sample, respectively. Since the sample was kept at the melting point, the heat input results in phase change. It can be seen in the figure that the heat flux is very large and decreases rapidly during the initial stage of melting. As the melting process progresses, variation of the heat flux becomes

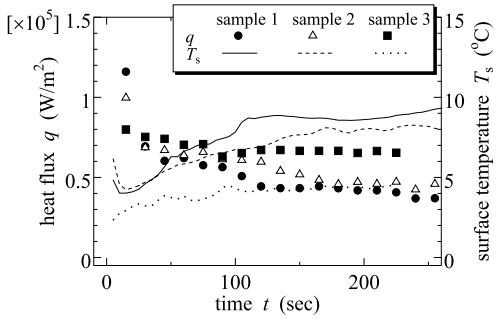

Fig. 8. Time dependencies of the heat flux and the surface temperature.

smaller. Since the melted liquid permeates into the solid rapidly due to the capillary effect, the thickness of the liquid film remains thin. Hence, the heat flux is large, and decreases with time due to a decrease of the capillary effect. The phenomenon is found to be more evident for smaller particle size. In the experiment, it was observed that the melted liquid does not flow out through the side of the porous material, in the case of sample 1, until the permeation layer reaches the top of the sample. Therefore, it was found that most of the melted liquid permeated into the porous material. After the initial state of the melting, it is found that the heat flux is larger for larger diameter particles despite the lower surface temperature. Since the permeability increases with the diameter of the particle, the melted liquid can be sucked smoothly into the material. Therefore, the liquid film becomes thinner and the higher heat flux can be obtained.

Fig. 9 shows time dependencies of the heat flux and the surface temperature for sample 4, 5 and 6. In the case of the larger particles, it is found that the variation of the heat flux is small compared with the sample consisting of smaller particles, and the melting process progresses almost in a quasi-steady state. This is because the unsteady effect decreases with decreasing capillary effect. Moreover, it is found that the heat flux decreases with increasing particle diameter, although the surface temperature rises with increasing diameter.

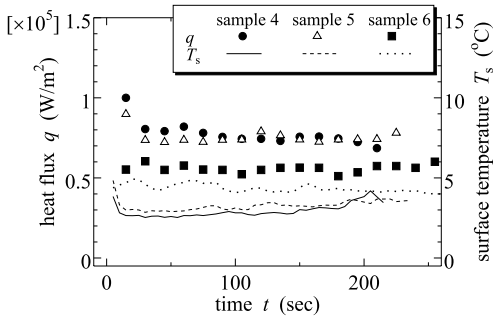

Fig. 9. Time dependencies of the heat flux and the surface temperature.

4.2. Comparison between experimental and analytical results

Fig. 10 shows time dependence of the heat flux in the case of sample 1. The analytical result was obtained from the melting model considering the total cross-section of the sample mentioned in Section 3.1. In the analytical result, there is a rapid drop at about 50 s. This is because there is a discontinuity of boundary conditions at the time, where the melting process shifts from situation 1 to situation 2, as shown in Fig. 6. The experimental and analytical results agree well and it is found that the analytical model is appropriate for the melting process of the porous material consisting of the particles that are smaller than 0.5 mm.

Fig. 11 shows time dependency of the heat flux in the cases of sample 4 and 6. The analytical result was obtained from the melting model considering the individual particles mentioned in Section 3.2. The experimental

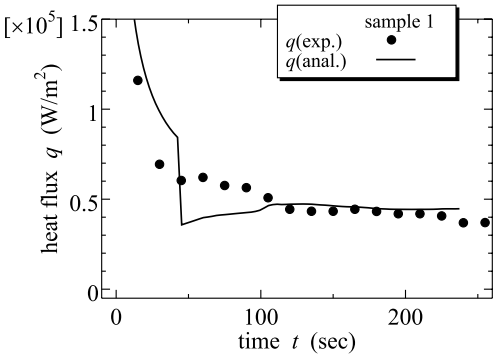

Fig. 10. Comparison between experimental and calculated heat flux (for sample 1).

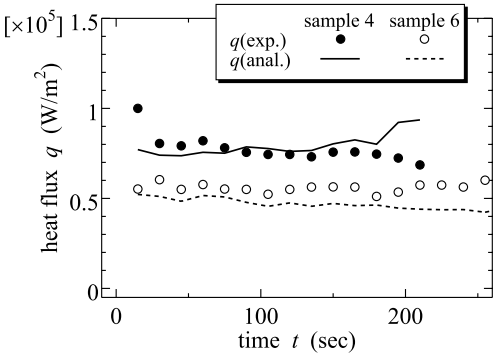

Fig. 11. Comparison between experimental and calculated heat flux (for samples 4 and 6).

and analytical results are in good agreement for each sample. Therefore, it is found that direct contact melting occurs independently around the individual particles in the case of large particles. In the present study, the melting process can be treated as an assembly of the direct contact melting of the individual particles for a porous material consisting of particles larger than about 4 mm. But, good agreement with the analytical results could not be obtained for samples whose particle diameters are from 0.5 to 2.8 mm. It seems that a melting process of these samples can be represented as a composite of the two models.

Fig. 12 shows a conceptual diagram of a relation between the heat flux and the particle diameter in the quasi-steady state, when the porosity, the average pressure and the surface temperature are set constant. In the case of a small particle, it is difficult for melted liquid to flow out through the porous material due to the small permeability, and most of the melted liquid is discharged through the liquid film. Therefore, it can be considered that the melting process is close to the direct contact melting of a dense sample. The heat flux increases with the particle diameter, because the melted liquid easily flows out through the porous material due to increasing permeability and the liquid film becomes thinner. That is to say, the heat flux is dominated by the permeability in the range where the process can be treated as the melting of the whole sample. When the permeability increases further with the particle diameter, the process shifts to the direct contact melting for the individual particles. In past studies [3,4], it was found that the thickness of the liquid film became larger by increasing diameter of the PCM. In this study, an average force acting on the particle increases with the particle diameter, because the number of the particles decreases. But, it is found that the effect of the particle diameter is stronger than that of the average force. Therefore, the heat flux decreases as the particle diameter is increased. Namely, the heat flux is dominated by the particle diameter in the case of the large diameter of the particle.

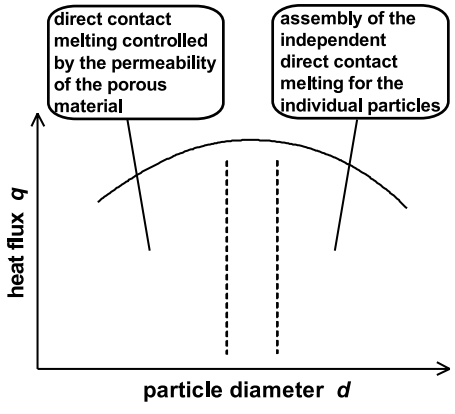

Fig. 12. Heat flux and the controlling phenomena in the quasi-steady state due to the particle diameter variation.

It seems that an applicable range of each model varies with other parameters, such as the radius of the sample, the porosity and so on. In the present study, when the particle diameter is smaller than 0.5 mm, the melting process can be treated as the melting process of the whole porous material, and the direct contact melting for the individual particles occurs when the diameter is larger than about 4 mm. Moreover, the composite melting process exists in the middle range where the particle size is from 0.5 to 4.0 mm.

5. Conclusion

The direct contact melting of a porous material was investigated experimentally and analytically. As a result, it was found that the heat flux at quasi-steady state increases with the particle diameter in the case of a small particles since the melting process is dominated by the permeability of the porous material. When the particle diameter is much larger, the melting process shifts to one in which the direct contact melting can be modeled by the individual particles and the heat flux decreases as the particle diameter increases. In analysis, two analytical models were proposed. One was calculated as the direct contact melting of the whole sample considering the total cross-section of the porous material, and another was treated as the assembly of the direct contact melting of the individual particles. The experimental and analytical results agree well with each other in the applicable range of each model.

Acknowledgements

The authors acknowledge the financial support of the Japan Society for the Promotion of Science under the project name of Research for the Future (JSPS-RFTF 97P01003, Fundamental Research on Thermal Energy Storage to Preserve Environment).

References

[1] D.A. Kearns, O.A. Plumb, Direct contact melting of a packed bed, Trans. ASME J. Heat Transfer 117 (1995) 452–457.
[2] K. Aoki, M. Hattori, T. Ujiie, A study of snow melting by heating from the bottom surface, Trans. JSME 53 (495) (1987) 3352–3357.
[3] A. Saito, Y. Utaka, M. Akiyoshi, K. Katayama, On the contact heat transfer with melting (1st report), Bull. JSME 28 (240) (1985) 1142–1149.

[4] A. Saito, Y. Utaka, M. Akiyoshi, K. Katayama, On the contact heat transfer with melting (2nd report), Bull. JSME 28 (242) (1985) 1703–1709.
[5] A. Saito, Y. Utaka, K. Shinoda, K. Katayama, Basic research on the latent heat thermal energy storage utilizing the contact melting phenomena, Bull. JSME 29 (255) (1986) 2946–2952.
[6] M.K. Moallemi, B.W. Webb, R. Viskanta, An experimental and analytical study of close-contact melting, ASME J. Heat Transfer 108 (1986) 894–899.
[7] T. Delker, D.B. Pengra, P. Wong, Interface pinning and the dynamics of capillary rise in porous media, Phys. Rev. Lett. 76 (6) (1996) 2902–2905.